Macromolecular Research, Vol. 17, No. 11, pp 879-885 (2009)

Reactive Hot Melt Polyurethane Adhesives Modified by Acrylic Copolymer Nanocomposites

Youn Bok Cho and Han Mo Jeong*

Department of Chemistry, University of Ulsan, Ulsan 680-749, Korea

Byung Kyu Kim

Department of Polymer Science and Engineering, Pusan National University, Busan 609-735, Korea

Received March 18, 2009; Revised April 21, 2009; Accepted April 21, 2009

Abstract: A macroazoinitiator (MAI) containing a poly(ethylene glycol) (PEG) segment was intercalated in the gallery of sodium montmorillonite (Na-MMT). Acrylic monomers were polymerized using this MAI intercalated in Na-MMT to prepare the acrylic copolymer nanocomposite (AN), which is a multiblock copolymer composed of two segments, an acrylic copolymer and PEG intercalated in Na-MMT (Na-MMT/PEG). When AN was used to modify the reactive hot melt polyurethane adhesive (RHA), the acrylic copolymer segment and Na-MMT/PEG synergistically enhanced the initial bond strength evolution and reduced the set time, even when the amount of Na-MMT in RHA was < 1 wt%. The viscosity of RHA increased and the tensile properties of the cured RHA film decreased due to modification with AN. These variations were more evident as the Na-MMT content in AN was increased.

Keywords: polyurethane, reactive hot melt adhesive, acrylic copolymer, Na-MMT, bond strength.

Introduction

The majority of reactive hot melt adhesives (RHA) are composed of isocyanate-terminated polyurethane (PU) prepolymer, which are applied in molten form, cooled to solidify, and subsequently cured by the reaction with ambient moisture.[1-3] This adhesive combines the merits of hot melt adhesive and traditional liquid curing adhesive, because the fast initial green bond strength can be developed by solidification upon cooling, and it can generate a higher final bond strength by the following curing reaction. That is, the residual isocyanate group reacts with moisture to form carbamic acid. This unstable carbamic acid decomposes into carbon dioxide and an amine. The amine reacts with isocyanate group to form an urea linkage.[4,5] Therefore, the final cured adhesive is a crosslinked material with an excellent bond strength and physical properties, including thermal and chemical resistances.

In certain applications, such as a high-speed continuous adhesion process, fast development of high green bond strength is advantageous, since the joined assemblies can be manufactured with high productivity. However, PU prepolymer of RHA normally has an average molecular weight of several thousands for easy handling and facile applications. Accordingly, various methods have been suggested to improve the initial bond strength of RHA. Acrylic polymers with high glass transition temperature or crystalline aliphatic polyester polyols are typical modifiers that can accelerate solidification and, consequently, initial bond strength development.[4,6-10]

Polymer/layered silicate nanocomposites exhibit markedly improved properties compared to pure polymers or conventional composites, because their unique intercalated or exfoliated structures maximize the interfacial contact between the organic polymer and layered silicate such as montmorillonite, which is composed of stacks of parallel lamellae with a 1 nm thickness and a high aspect ratio. In the nanocomposites, the segmental motions of the polymer chains are restricted due to the confinement of the polymer chains between the silicate layers as well as by the silicate surface-polymer interaction in the nano-structured composites.[11-18] These observations suggest that the solidification which occurs by the cooling of the polymer melt can be enhanced by the presence of a layered silicate.[19,20]

The poly(ethylene glycol) (PEG) segment can be easily intercalated in the sodium montmorillonite (Na-MMT) gallery. The Na-MMT intercalated with PEG (Na-MMT/PEG) has high stability because the intercalated PEG cannot be easily washed out after intercalation, even with solvents which have high affinity toward Na-MMT.[21,22] Therefore, it can be anticipated that a macroazoinitiator (MAI) containing a

*Corresponding Author. E-mail: hmjeong@mail.ulsan.ac.kr

poly(ethylene glycol) (PEG) segment, as shown in the following chemical structure, can be easily intercalated at the gallery of Na-MMT. This can be utilized in the radical polymerization of acrylic monomers in order to prepare the multiblock copolymer of Na-MMT/PEG and acrylic copolymer.[23-25]

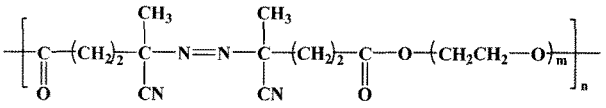

In this study, we prepared the multiblock copolymers and utilized them as modifiers of RHA because we expected that finely dispersed Na-MMT/PEG block and acrylic copolymer block can synergistically enhance the solidification and the consequent initial bond strength development after application. The bond strengths and the rheological, mechanical properties of the modified RHA were examined and compared with those of pristine RHA.

Experimental

Materials. Isobornyl acrylate (IBA, Aldrich), 2-ethylhexyl acrylate (EHA, Tokyo Kasei), methacrylic acid (MAA, Tokyo Kasei), 2,2'-azobisisobutyronitrile (AIBN, Junsei Chemicals), macroazoinitiator (MAI, Wako Pure Chemical, VPE-0201), *n*-dodecyl mercaptan (DMC, Aldrich), acetonitrile (Aldrich), methanol (Aldrich) and tetrahydrofuran (THF, Aldrich) were used as received. The MAI was the condensation polymer of 4,4'-azobis(4-cyanopentanoic acid) and PEG, whose molecular weight was 2,000. The molecular weight of MAI suggested by the supplier was about 20,000, and its azo group content was 0.45 mmol/g. Na-MMT (Southern Clay) was used after drying at 60 °C in a vacuum oven for 2 days. Two types of poly(propylene glycol) (PPG), PPG-3000 (molecular weight: 3,000) and PPG-1000 (molecular weight: 1,000) were obtained from BASF Korea and Korea Polyol, respectively. The crystalline polyester polyols, Dynacoll-7360 (molecular weight: 3,500; melting temperature: 55 °C) and Dynacoll-7381 (molecular weight: 3,500; melting temperatue: 65 °C) were supplied from Degussa. A nonpolar hydrogenated polybutadiene polyol (Polytail-H, molecular weight: 3,000~4,000; OH value: 44±5, melting temperature: 60~70 °C) was the product of Mitsubishi Chemical. Liquid methylene diphenyl diisocyanate (MDI) containing 50% *para, para'*-MDI and 50% *ortho, para'*-MDI was obtained from BASF Korea. The catalyst, 2,2'-dimorpholinoethyl ether (DMEE, Huntsman) was used as received.

Preparation. Na-MMT intercalated with MAI (Na-MMT/MAI) was prepared using an acetonitrile/methanol mixture (1/1 by volume) as a solvent.[21,22] That is, 3 g of MAI were dissolved in 100 mL of solvent and the solution was stirred with 7 g of Na-MMT for 1 day at room temperature. The intercalated compound was separated with a centrifuge and repeatedly washed with acetonitrile and methanol to remove non-intercalated physisorbed MAI. It was then dried at 25 °C for 48 h under vacuum before use. The amount of MAI intercalated at the gallery of Na-MMT, determined by thermogravimetry, was 0.18 g-MAI/g-Na-MMT.

Acrylic copolymer nanocomposites (AN) were prepared by the radical copolymerization of IBA, EHA, and MAA with Na-MMT/MAI and/or AIBN in THF in the presence of the chain transfer agent, DMC, at 70 °C for 5 h. The relative amounts of AIBN and MAI, as shown in the recipes in Table I, were adjusted so that the total azo group in the polymerization mixture was the same amount, 3 mmol. The polymerization yields after evaporating THF and the residual monomers at room temperature in a vacuum oven for 1 day were more than 99% for all the samples. The properties of the acrylic copolymer nanocomposites are shown in Table II.

A 1 L round-bottomed, four-necked flask equipped with a mechanical stirrer, a thermometer, a nitrogen gas inlet, and a condenser with a drying tube was used as the reaction vessel, and the reaction temperature was controlled with an oil bath. The recipes for the preparation of RHAs are shown in Table III. The total feed weight of RHA-0 except DMEE

Table II. Properties of Acrylic Copolymer Nanocomposites

Sample	Molecular Weight		T_g (°C)
	M_n	M_w	
AN-0	5,241	10,363	70
AN-1	5,484	10,661	73
AN-3	5,241	10,151	73
AN-5	4,892	9,712	73

Table I. Recipes for the Preparation of Acrylic Copolymer Nanocomposites

Designation	Feed Composition (g)						
	Monomer			Initiator		Chain Transfer Agent	Solvent
	IBA	EHA	MAA	AIBN	Na-MMT / MAI	DMC	THF
AN-0	82	9	9	0.454	-	1.36	91
AN-1	82	9	9	0.445	0.773 / 0.136	1.36	91
AN-3	82	9	9	0.418	2.309 / 0.418	1.36	91
AN-5	82	9	9	0.391	3.855 / 0.691	1.36	91

Table III. Recipes for the Preparation of RHAs

Sample	Feed (g)								
	PPG-1000	PPG-3000	Dynacoll-7360	Dynacoll-7381	Potail-H	AN		MDI	DMEE
						Kind	Amount		
RHA-0	17.90	17.90	17.90	17.90	10.00	-		18.40	0.125
RHAN-0	17.90	17.90	17.90	17.90	10.00	AN-0	21.86	18.40	0.125
RHAN-1	17.90	17.90	17.90	17.90	10.00	AN-1	21.86	18.40	0.125
RHAN-3	17.90	17.90	17.90	17.90	10.00	AN-3	21.86	18.40	0.125
RHAN-5	17.90	17.90	17.90	17.90	10.00	NA-5	21.86	18.40	0.125

was 100 g, and additional 21.86 g of AN was fed as a modifier in RHAN-0 ~ RHAN-5. First, MDI was reacted with Polytail-H for 2 h at 90 °C, and then the other polyols, AN, and DMEE were fed into the vessel and reacted further for 4 h at 90 °C to prepare an isocyanate-terminated PU prepolymer. After the reaction, the RHA was degassed in the reactor for 1 h at 90 °C with a vacuum pump. The isocyanate group content and the molecular weight of the PU prepolymer were designed in the recipes to be 6.2 wt% and 2,780, respectively.

Characterization. The number average molecular weight (M_n) and the weight average molecular weight (M_w) of acrylic copolymer were measured at 43 °C with gel permeation chromatography (GPC, Waters M510). The copolymers were dissolved in THF and the solution was filtered with a 0.45 μm membrane filter before measurement. THF was used as an eluent.

X-ray diffraction (XRD) patterns were obtained with an X-ray diffractometer (Rigaku, RAD-3C) using CuK_α radiation (λ=1.548 Å) as the X-ray source. The diffraction angle was scanned from 1.0° at a rate of 1.2°/min.

The melt viscosity of RHAs was measured using a Brookfield viscometer (DV-11Pro) with a spindle (SC4-27) rotating at 20 rpm at 100 °C or 120 °C. The growth of melt viscosity after 1 h at 120 °C was compared to the initial viscosity, which was used as the metric for viscosity stability.

Dynamic rheological properties were measured with a cone and plate rheometer (Physica, MCR 301) at 120 °C and 15% strain level. The cone angle and the diameter of the plate were 1.0° and 50 mm, respectively.

Tensile tests were performed with a tensile tester (Shimadzu AGS-1000D, Japan) according to the ASTM D882 standard. The dumbbell shaped micro-tensile specimen had the following dimensions: 100 mm in length, 10 mm in width, and a thickness of 0.2 mm. The specimen was elongated at a rate of 200 mm/min. The film for this test was obtained by curing the RHA at 30 °C in a 50% relative humidity environment for 3 days.

The dynamic mechanical properties of the 0.2 mm thick cast films were analyzed using a dynamic mechanical analyzer (DMA, TA Instrument, DMA-Q800). Testing was performed in bending mode at 1 Hz with a heating rate of 5 °C/min.

Differential scanning calorimetry (DSC) (DSC 823^e, Mettler Toledo) was conducted at a heating and cooling rate of 10 °C/min with 7 mg of sample. The samples were loaded at 30 °C. The melting temperature (T_m) and the heat of fusion (ΔH_m) of cured RHA films were measured on a first heating scan. The acrylic copolymers were cooled down to 30 °C after heating to 150 °C, and the glass transition temperature (T_g) was measured in a subsequent second heating scan.

A PPF sheet, which is the composite of polypropylene, ethylene-propylene rubber, talc, and other minor components, was treated with plasma to have a surface tension of 40 dyne/cm. This sheet was coated with RHA melted at 120 °C to a thickness of 0.2 mm. Then PU foam (2 mm thick, 10 mm in width, and 50 mm in length) was brought in contact with the sheet and pressed with a 5 kg roller, and allowed to stand at 30 °C in a 50% relative humidity environment. The bond strengths after 10 min, 30 min, and 3 days were measured by a 180° peel test with a push-pull gauge (Imada, DPS-50, Japan) at a peel rate of about 20 mm/min.

The set time was measured according to the method suggested by Degussa. Briefly, approximately 0.58 mg/mm^2 of RHA at 120 °C was applied to the wide side of a wooden block whose dimensions were 113 mm in width, 22 mm in length, and 6 mm in height. A second block was attached to the first one and carefully twisted. The set time was defined as the time when the cubes could no longer be twisted.

Results and Discussion

XRD. In Figure 1, the XRD pattern of Na-MMT has a peak at 2θ=7.7°, whereas Na-MMT/MAI has a peak at 2θ=5.1°. These results show that the basal plane spacing d_{001}, which was calculated by Bragg's law, where $d_{001}=\lambda/(2 \sin \theta)$, increased from 11.5 Å to 17.3 Å by the intercalation of MAI. Considering that the thickness of the silicate layer alone is approximately 9.5 Å,[26] one can see that the results of Figure 1 suggest that the interlayer distance of Na-MMT/MAI is 7.8 Å (17.3-9.5=7.8). Similarly, many researchers reported that the interlayer distance was about 8 Å, when

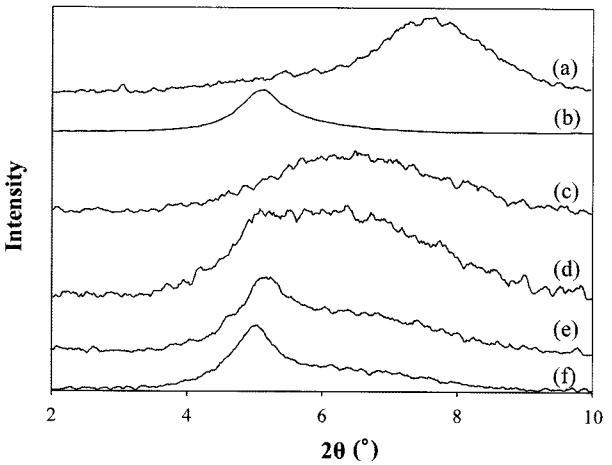

Figure 1. XRD pattens of (a) Na-MMT, (b) Na-MMT/MAI, (c) AN-0, (d) AN-1, (e) AN-3, and (f) AN-5.

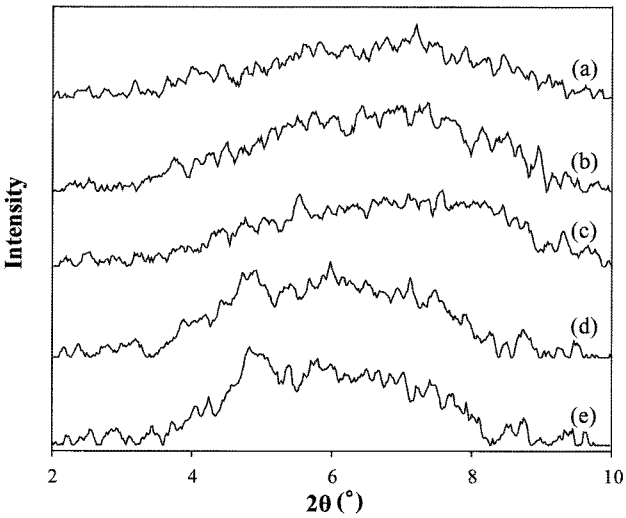

Figure 2. XRD patterns of (a) RHA-0, (b) RHAN-0, (c) RHAN-1, (d) RHAN-3, and (e) RHAN-5.

PEG, whose molecular weight was higher than 2,000, was intercalated in the gallery of Na-MMT. Two kinds of models, helical conformation or double layer planar zigzag disposition, were suggested to explain the intercalated structure.[21,22,26]

The XRD patterns of AN-1, AN-3, and AN-5 have a peak at 2θ=5.1°, 5.2°, and 5.0°, respectively. These results that Na-MMT/MAI and ANs have the XRD peaks at similar positions suggest that the structure of Na-MMT intercalated with PEG in Na-MMT/MAI does not vary, even after the polymerization of acrylic monomers.

Figures 2(d) and (e) show that RHAN-3 and RHAN-5 have a peak at 2θ=4.9° and 4.8°, respectively. These peak positions are almost similar with those of Na-MMT/MAI and ANs, although slightly moved to lower angle. This result shows that the structure of Na-MMT intercalated with PEG is retained in RHA, but is further expanded by the additional intercalation of other segments of RHA.

Rheological Properties. The steady shear viscosity of RHA measured by a Brookfield viscometer is shown in Table IV. Normally, commercial RHA has the viscosity value in the range of 5~20 Pa·s at the application temperature.[27] Compared to these values, the RHA-0 has lower viscosity, even at 100 °C. The viscosity is evidently increased in RHAN-0 by the addition of acrylic copolymer, because the acrylic copolymer has a higher molecular weight and a higher T_g. This viscosity is further increased when the content of Na-MMT in the acrylic copolymer is increased, as normally observed in the nanocomposites due to the interactions between matrix polymer and nano-filler, although the content of Na-MMT in the RHAN-1, RHAN-3 and RHAN-5 are only 0.14, 0.41 and 0.68 wt%, respectively.[27]

The temperature dependency of viscosity is a factor that should be considered for the practical utilization of an RHA; low viscosity at the time of application is a desirable attribute for ease of processing, and development of early viscosity during cooling can improve the initial bond strength for a fast set. Table IV shows the activation energy for flow, E, calculated by eq. (1), where R is the gas constant. E increases when RHA is modified with acrylic copolymers; however, the content of MMT in the acrylic copolymer does not considerably affect the value of E.

$$\ln\frac{\eta_{373}}{\eta_{393}} = \frac{E}{R}\left(\frac{1}{373}-\frac{1}{393}\right) \quad (1)$$

The stability of the melt viscosity at the application tem-

Table IV. Physical Properties of RHAs

Sample	Melt Viscosity (Pa·s)		E (kJ/mol)	Viscosity Growth at 120 °C (%/h)	Thermal Properties	
	100 °C	120 °C			T_m (°C)	ΔH_m (J/g)
RHA-0	3.61	1.95	37.6	6.7	57.9	45.1
RHAN-0	9.69	4.29	49.6	15.9	56.7	36.2
RHAN-1	9.86	4.30	50.5	15.1	56.4	37.7
RHAN-3	10.16	4.50	49.7	15.2	55.1	35.5
RHAN-5	11.05	5.20	45.9	13.5	57.7	35.7

perature is a factor that must be evaluated in the practical applicability of an RHA. The growth of viscosity for 1 h at 120 °C under a constant shear rate by a spindle rotating at 20 rpm is shown in Table IV. The increased viscosity growth by modification with acrylic copolymer nanocomposites is somewhat different from those of our previous report, where the viscosity stability was improved with the addition of acrylic copolymer.[6,28] When one consider the fact that the acrylic copolymers used in this study have a MAA unit, whereas those used in our previous studies do not, this viscosity instability seems to be caused by the presence of a MAA unit, because the carboxylic acid group of MAA can react with the isocyanate group of PU prepolymer.

The complex viscosity, η^* of RHA is shown in Figure 3, which demonstrates that RHA-0 exhibits Newtonian fluid behavior. There is a plateau of constant η^*, independent of the frequency of oscillation (ω), which persisted up to ω= 100 rad/s. This behavior shows that the molecular weight of the RHA constituents were not high enough to induce the shear thinning behavior observed in polymers which have a polydispersity of molecular weights. Figure 3 shows that the η^* is increased when ANs are added as a modifier, and this increase is more evident as the content of Na-MMT in the AN is increased. In addition, mild non-Newtonian shear thinning behavior, where η^* decreased with increasing shear rate, is observed at a low shear rate. This particular phenomenon at a low shear rate is more clearly represented in Figure 4 due to the higher sensitivity of storage shear modulus, G', to morphological state.[29-31] That is, Figure 4 shows that G' increases compared to that of RHA-0, and that this increase of G' is more evident at a low shear rate so that the frequency dependency of G' is reduced, as the content of Na-MMT in the AN is increased. In the case of RHA-0, the log G' increased linearly with a slope of 1.73 when log ω increased. However, a reduction of this slope, i.e., non-terminal behavior, is observed at low shear rate when ANs are

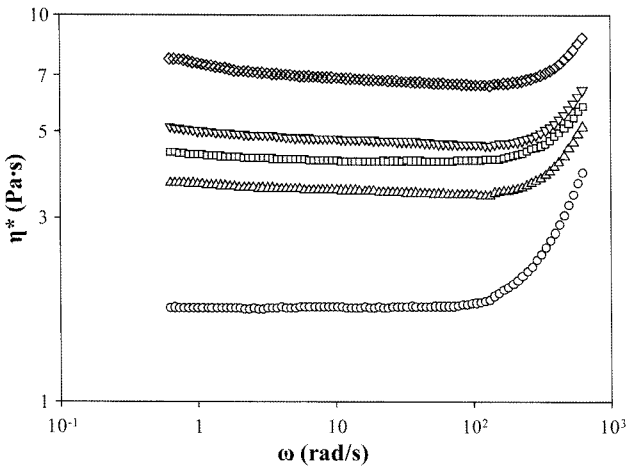

Figure 3. Complex viscosity versus frequency of (○) RHA-0, (△) RHAN-0, (□) RHAN-1, (▽) RHAN-3, and (◇) RHAN-5.

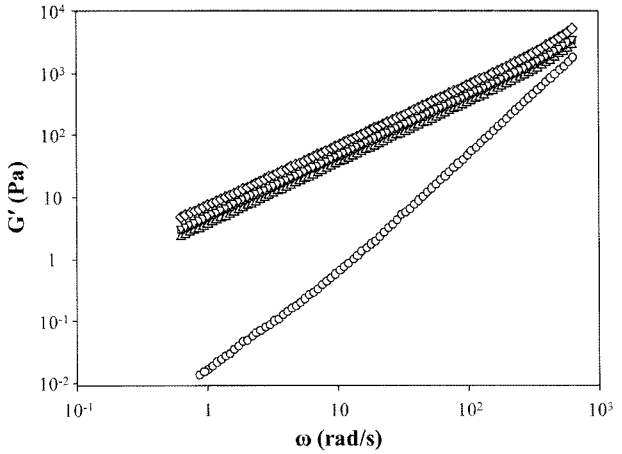

Figure 4. Storage shear modulus versus frequence of (○) RHA-0, (△) RHAN-0, (□) RHAN-1, (▽) RHAN-3, and (◇) RHAN-5.

added. This diminished frequency dependence of G' at low shear rate suggests the possibility of pseudo-solid like behavior that may be attributed to incomplete relaxation. Incomplete relaxation of dispersed Na-MMT can be caused by the physical congestion of highly anisotropic silicate layers, which prevents free rotation in compliance with external dynamic shear. This incomplete relaxation and interaction between the silicate layers can create a three-dimensional mesoscopic structure of silicate layer, making the silicate layers unable to independently relax, which in turn cause the observed pseudo-solid like behavior.[32] The increase of η^* and the diminished frequency dependence of G' at low frequency may also be attributed to the slower relaxation of matrix molecules due to strong interaction between silicate layers and RHA molecules.[33,34] Therefore, this onset of pseudo-solid behavior even with very small quantities of Na-MMT demonstrates that the Na-MMT is finely dispersed in the RHA matrix.

The rise of η^* at high shear rate range above 100 rad/s in Figure 3 suggests that the viscosity growth due to chain extension reaction is occurring at this shear rate range by high shear force, as one observed in the viscosity growth for 1 h at 120 °C under a constant shear rate by a spindle rotating at 20 rpm, as shown in Table IV.

Physical Properties and Bond Strength. Table IV shows that the T_m of the aliphatic polyester segment does vary significantly by the addition of ANs. However, the ΔH_m is decreased by the modification with ANs compared to that of RHA-0, although the effect of Na-MMT content on ΔH_m is not clearly observed. This effect shows that the crystallization of the aliphatic polyester segment is hindered by the ANs, whereas the effect of Na-MMT is not significant.

In Table V, the tensile modulus of RHAN-0 is increased compared to that of RHA-0 by the addition of AN-0, which has a more rigid chain structure compared to those of polyols. However, the modulus decreases as the content of Na-

Table V. Tensile and Adhesion Properties of RHAs

Sample	Tensile Properties			Set Time	Bond Strength (N/m) Over Time		
	Modulus (MPa)	Tensile Strength (MPa)	Elongation at Break (%)		10 min	30 min	3 day
RHA-0	141±12	18.72±1.69	829±45	12 min 30 s	157	196	Fracture
RHAN-0	158±13	9.72±1.66	485±70	4 min 15 s	186	226	Fracture
RHAN-1	146±4	9.70±1.15	393±28	2 min 20 s	206	235	Fracture
RHAN-3	134±2	7.69±0.72	329±38	2 min 30 s	245	265	Fracture
RHAN-5	112±1	5.35±0.04	113±36	2 min 35 s	353	363	Fracture

MMT in the ANs is increased, and the tensile strength and the elongation at break are reduced by the modification with ANs, more evidently as the content of Na-MMT in AN is increased. These abnormal results, which include the reduction of tensile properties in the presence of more rigid acrylic copolymer and nano-filler, suggest the possibility that the degree of crosslinking of the RHA film is reduced, as in our previous studies.[19,28] That is, as observed in the rheological properties, the chain mobility is reduced by the presence of acrylic copolymer and Na-MMT, which restricts the reactions between the chain end.

The storage tensile modulus (E') of cured film measured by DMA is shown in Figure 5. The E' of RHA-0 decreases slowly upon heating from -150 °C because of thermal expansion. This E' reduction becomes evident at T_g, and another sudden drop of E' occurs at T_m. Figure 5 shows that this E' at all temperature ranges below T_m is increased by the modification with AN-0, and then decreased again by the modification with AN-3 and AN-5, as the tensile modulus in Table V varies. These results also show that the degree of crosslinking of RHA film is reduced by the restricted chain mobility in the presence of acrylic copolymer and Na-MMT.

Table V shows that the set time is reduced dramatically by the addition of AN-0 compared to that of RHA-0, and this is further decreased when modified with AN-1. These results show that acrylic copolymer and Na-MMT can reduce the set time synergistically, even when the content of Na-MMT in RHA is only 0.14 wt%. However, this set time was not reduced more by the increased amount of Na-MMT, as shown in Table V, which shows that the effect of Na-MMT on set time is saturated at a very low content. This shows that AN-1 can be used as an effective modifier of RHA for fast set with minor viscosity increase.

Table V also shows that the initial bond strength up to 30 min is improved by the addition of acrylic copolymer, and this enhancement is amplified by Na-MMT. The enhanced solidification due to diminished chain mobility caused by ANs can be suggested as a cause of this early development of bond strength. In Table V, "Fracture" means that fracture had occurred not at RHA layer but at PU foam.

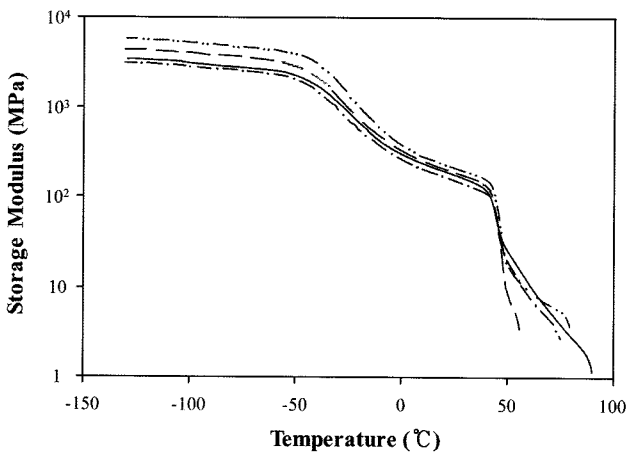

Figure 5. Storage tensile modulus of (——) RHA-0, (–··–) RHAN-0, (——) RHAN-3, and (- · · · -) RHAN-5.

Conclusions

Our experimental results showed that acrylic copolymer nanocomposites can effectively accelerate the setting and the initial bond strength development of RHA by the synergistic contribution of a high T_g acrylic copolymer segment and Na-MMT intercalated with PEG segment. However, the tensile properties of the cured film were reduced by the addition of acrylic copolymer nanocomposites. This reduction was more evident as the content of Na-MMT in the acrylic copolymer nanocomposite was increased. These results suggest that the the crosslinking reaction between the chain end is hindered by acrylic copolymer nanocomposites, because they increase the viscosity of RHA and consequently reduce the mobility of the chain end.

Acknowledgements. This research was supported by the regional industry promotion program of The Ministry of Knowledge Economy of the Korean Government (Grant Number: 10018023).

References

(1) R. De Genova, M. D. Harper, W. A. Clay, P. E. Cranley, and M. K. Hunter, *Tappi J.*, **79**, 196 (1996).
(2) P. Waites, *Pigment Resin Technol.*, **26**, 300 (1997).

(3) J.-M. Hung, *Proceeding of the Hot Melt Symposium*, Hilton Head Island, SC, June 10-13, p 91 (2001).
(4) Y. Cui, D. Chen, X. Wang, and X. Tang, *Int. J. Adhes. Adhes.*, **22**, 317 (2002).
(5) Y. Cui, L. Hong, X. Wang, and X. Tang, *J. Appl. Polym. Sci.*, **89**, 2708 (2003).
(6) J. S. Jung, J. H. Kim, M. S. Kim, H. M. Jeong, Y. S. Kim, T. K. Kim, J. M. Hwang, S. Y. Lee, and Y. L. Cho, *J. Appl. Polym. Sci.*, **109**, 1757 (2008).
(7) J. M. Hung, W. K. Chu, and Y. S. Zhang, US Patent 0072953 (2004).
(8) D. T. Rumack, US Patent 0010443 (2003).
(9) J.-M. Hung, J. W. Nowicki, G. A. Hespe, and P. P. Puletti, US Patent 5866656 (1999).
(10) J. W. Nowicki and R. S. Wallach, US Patent 5939488 (1999).
(11) H. U. Jeon, D. H. Lee, D.-J. Choi, M. S. Kim, J. H. Kim, and H. M. Jeong, *J. Macromol. Sci. -Phys.*, **46**, 1151 (2007).
(12) K. H. Kim, K. H. Kim, J. H. Huh, and W. H. Jo, *Macromol. Res.*, **15**, 178 (2007).
(13) J.-C. Kim and J.-H. Chang, *Macromol. Res.*, **15**, 449 (2007).
(14) W. Kim, S. K. Kim, J.-H. Kang, Y. Choe, and Y.-W. Chang, *Macromol. Res.*, **14**, 187 (2006).
(15) J. H. Park, W. N. Kim, H.-S. Kye, S.-S. Lee, M. Park, J. Kim, and S. Lim, *Macromol. Res.*, **13**, 367 (2005).
(16) S. B. Oh, B. S. Kim, and J.-H. Kim, *J. Ind. Eng. Chem.*, **12**, 275 (2006).
(17) S. S. Ray, *J. Ind. Eng. Chem.*, **12**, 811 (2006).
(18) F. F. Fang and H. J. Choi, *J. Ind. Eng. Chem.*, **12**, 843 (2006).
(19) H. M. Jeong, D. H. Kim, J. S. Jung, T. K. Kim, B. K. Kim, Y. S. Kim, Y. L. Cho, and J. M. Hwang, *Compos. Interfaces*, **14**, 467 (2007).
(20) H. M. Jeong, D. H. Kim, K. S. Yoon, J. S. Jung, Y. S. Kim, T. K. Kim, Y. L. Cho, and J. M. Hwang, *J. Adhes. Sci. Technol.*, **21**, 841 (2007).
(21) P. Aranda and E. Ruiz-Hitzky, *Chem. Mater.*, **4**, 1395 (1992).
(22) J. Wu and M. M. Lerner, *Chem. Mater.*, **5**, 835 (1993).
(23) A. Ueda and S. Nagai, *J. Polym. Sci. Part A: Polym. Chem.*, **24**, 405 (1986).
(24) H. M. Jeong, M. Y. Choi, and Y. T. Ahn, *Macromol. Res.*, **14**, 312 (2006).
(25) M. S. Kim, J. K. Jun, and H. M. Jeong, *Compos. Sci. Technol.*, **68**, 1919 (2008).
(26) E. Ruiz-Hitzky and P. Aranda, *Adv. Mater.*, **2**, 545 (1990).
(27) R. De Genova, L. Grier, D. P. Murray, and W. Clay, *Polymers, Laminations, & Coatings Conference*, **1**, 285 (1997).
(28) J. H. Kim, M. S. Kim, H. M. Jeong, Y. S. Kim, T. K. Kim, J. M. Hwang, S. Y. Lee, and Y. L. Cho, *Compos. Interfaces*, **15**, 577 (2008).
(29) T. J. Pinnavaia and G. W. Beall, Eds., *Polymer-Clay Nanocomposites*, Wiley, New York, 2000.
(30) L. A. Utracki, *Clay-Containing Polymeric Nanocomposites*, Rapra Technology Ltd, Shawbury, 2004.
(31) T. D. Fornes, P. J. Yoon, H. Keskkula, and D. R. Paul, *Polymer*, **42**, 9929 (2001).
(32) Y. H. Hyun, S. T. Lim, H. J. Choi, and M. S. Jhon, *Macromolecules*, **34**, 8084 (2001).
(33) R. Krishnamoorti and E. P. Giannelis, *Macromolecules*, **30**, 4097 (1997).
(34) Y. T. Lim and O. O. Park, *Rheol. Acta*, **40**, 220 (2001).